SLAC-PUB-12381
March 2007

The Conformal Template and New Perspectives for Quantum Chromodynamics

Stanley J. Brodsky

Stanford Linear Accelerator Center, Stanford University, Stanford, CA, 94309

Conformal symmetry provides a systematic approximation to QCD in both its perturbative and nonperturbative domains. One can use the AdS/CFT correspondence between Anti-de Sitter space and conformal gauge theories to obtain an analytically tractable approximation to QCD in the regime where the QCD coupling is large and constant. For example, there is an exact correspondence between the fifth-dimensional coordinate of AdS space and a specific impact variable which measures the separation of the quark constituents within the hadron in ordinary space-time. This connection allows one to compute the analytic form of the frame-independent light-front wavefunctions of mesons and baryons, the fundamental entities which encode hadron properties and allow the computation of exclusive scattering amplitudes. One can also use conformal symmetry as a template for perturbative QCD predictions where the effects of the nonzero beta function can be systematically included in the scale of the QCD coupling. This leads to fixing of the renormalization scale and commensurate scale relations which relate observables without scale or scheme ambiguity. The results are consistent with the renormalization group and the analytic connection of QCD to Abelian theory at $N_C \to 0$. I also discuss a number of novel phenomenological features of QCD. Initial- and final-state interactions from gluon-exchange, normally neglected in the parton model, have a profound effect in QCD hard-scattering reactions, leading to leading-twist single-spin asymmetries, diffractive deep inelastic scattering, diffractive hard hadronic reactions, the breakdown of the Lam Tung relation in Drell-Yan reactions, and nuclear shadowing and non-universal antishadowing—leading-twist physics not incorporated in the light-front wavefunctions of the target computed in isolation. I also discuss tests of hidden color in nuclear wavefunctions, the use of diffraction to materialize the Fock states of a hadronic projectile and test QCD color transparency, nonperturbative antisymmetric sea quark distributions, anomalous heavy quark effects, and the unexpected effects of direct higher-twist processes.

§1. Introduction

This unique conference has illuminated the historical path of the past 50 years which led to the development of quantum chromodynamics, starting with Sakata's $pn\Lambda$ proposal.[1] This model gave the first indication of $SU(3)$ flavor symmetry and ultimately, a composite theory of hadrons. The SLAC measurement of inelastic electron-proton scattering in 1969[2] demonstrated the Bjorken scale invariance[3] of the deep inelastic cross section and gave the first indications that the constituents of the proton are effectively pointlike, thus establishing Gell Mann,[4] Ne'eman[5] and Zweig's[6] quarks as elementary constituent fields on par with the leptonic fields of quantum electrodynamics. The application of Feynman's parton model by Bjorken and Paschos[7] and Drell, Levy and Yan[8] to deep inelastic lepton-proton scattering provided the basis for applying quantum field theory to the strong interactions. A crucial theoretical development was the advent of parastatistics by Greenberg[9] which solved the apparent contradiction of the quark model with the spin-statistics problem and provided the basis for $SU(3)$ gauge symmetry. These historical developments led

Invited talk presented at International Symposium On The Jubilee Of The Sakata Models (PnLambda50), 11/25/2006-11/26/2006, Nagoya, Japan

Work supported by US Department of Energy contract DE-AC02-76SF00515

to the development by Gell-Mann, Fritzsch and Leutwyler[10] of our present theory of quantum chromodynamics based on the exact non-Abelian Yang-Mills[11] $SU(3)$ local color gauge invariance. The alternative Han-Nambu model[12] with integral quark charges was ruled out by hard two-photon reactions.[13]

QCD is a fascinating theory with remarkable complexity and novel features. The physical mechanisms underlying color confinement are still being clarified. Experiments at RHIC[14] are now probing new phenomena associated with the high temperature phase of QCD where its quark and gluon degrees of freedom become explicit.

In this talk I will discuss how conformal symmetry can provide a systematic approximation to QCD in both its nonperturbative and perturbative domains. In the case of nonperturbative QCD, one can use the AdS/CFT correspondence[15] between Anti-de Sitter space and conformal gauge theories to obtain an analytically tractable approximation to QCD in the regime where the QCD coupling is large and constant. This connection allows one to compute the analytic form[16),17] of the frame-independent light-front wavefunctions of mesons and baryons, the fundamental entities which encode hadron properties and allow the computation of exclusive scattering amplitudes. One can also use conformal symmetry as a template[18] for perturbative QCD expansions where the effects of the nonzero QCD β-function can be systematically incorporated into the scale of the running coupling.[19)–21] This leads to fixing of the renormalization scale and commensurate scale relations which relate observables without scale or scheme ambiguity.[22] The results are consistent[23] with the renormalization group[24] and the analytic connection of QCD to Abelian theory at $N_C \to 0$.[25]

I will also review in this talk some novel features of QCD. For example, initial- and final-state interactions normally neglected in the parton model have a profound effect in QCD hard-scattering reactions, leading to leading-twist single-spin asymmetries, diffractive hard hadronic reactions, the breakdown of the Lam Tung relation in Drell-Yan reactions. Diffractive deep inelastic scattering leads the shadowing and antishadowing of nuclear structure functions—leading-twist physics not incorporated in the light-front wavefunctions of the target computed in isolation. I also will discuss tests of hidden color in nuclear wavefunctions, the use of diffraction to materialize the Fock states of a hadronic projectile and test QCD color transparency, nonperturbative antisymmetric sea quark distributions, anomalous heavy quark effects, and the unexpected effects of direct higher-twist processes. Many of these features of QCD can be tested at RHIC, e^+e^- colliders, Fermilab, and the new hadron physics facilities at JLAB, GSI-FAIR, and J-PARC.

§2. Analytic Connection of QCD to Abelian Theory

An important guide to perturbative QCD predictions is consistency in the $N_C \to 0$ limit where the theory becomes Abelian.[25] One can consider QCD predictions as analytic functions of the number of colors N_C and flavors N_F. Remarkably, one can show to all orders of perturbation theory[25] that PQCD predictions reduce to those of an Abelian theory similar to QED at $N_C \to 0$ with $C_F\alpha_s$ and $N_F/(T_F C_F)$ held

fixed, where $C_F = (N_C^2 - 1)/(2N_C)$ and $T_F = 1/2$. The resulting theory corresponds to the group $1/U(1)$ – not $U(1)$ Abelian QED. This means that light-by-light diagrams acquire a particular topological factor. The $N_C \to 0$ limit is complimentary to 't Hooft's large N_C limit; it provides an important check on the analytic behavior of QCD expressions: QCD formulae and phenomena must match their Abelian analog. In particular, the renormalization scale in perturbative expansions is effectively fixed[22] by this requirement.

§3. Infrared Fixed Point

The negative β function of the quark-gluon coupling at high virtuality implies asymptotic freedom and allows the perturbative analysis of both inclusive and exclusive hard scattering hadronic reactions. It has usually been assumed that the negative β QCD function also implies "infrared slavery"; i.e.; that the QCD coupling becomes singular in the infrared. However, solutions of the QCD Dyson Schwinger equations[26),27] and phenomenological studies[28)–30] of QCD couplings based on physical observables such as τ decay[31] suggest that the QCD β function vanishes and $\alpha_s(Q^2)$ become constant at small virtuality; *i.e.*, effective charges develop an infrared fixed point. Recent lattice gauge theory simulations[32] and nonperturbative analyses[33] have also indicated an infrared fixed point for QCD. One can understand this physically:[17] in a confining theory where gluons have an effective mass or maximal wavelength, all vacuum polarization corrections to the gluon self-energy decouple at long wavelength. When the coupling is constant and quark masses can be ignored, the QCD Lagrangian becomes conformally invariant,[34] allowing the mathematically tools of conformal symmetry to be applied, such as the AdS/CFT correspondence.[15]

§4. Perturbative QCD and Exclusive Processes

Exclusive processes provide an important window on QCD processes and the structure of hadrons. Rigorous statements can be made on the basis of asymptotic freedom and factorization theorems which separate the underlying hard quark and gluon subprocess amplitude from the nonperturbative physics of the hadronic wavefunctions. The leading-power contribution to exclusive hadronic amplitudes such as quarkonium decay, heavy hadron decay, and scattering amplitudes where hadrons are scattered with large momentum transfer can often be factorized as a convolution of distribution amplitudes $\phi_H(x_i, \Lambda)$ and hard-scattering quark/gluon scattering amplitudes T_H integrated over the light-front momentum fractions of the valence quarks:[35] $\mathcal{M}_{\rm Hadron} = \int \prod \phi_H^{(\Lambda)}(x_i, \lambda_i)\, T_H^{(\Lambda)} dx_i$. Here $T_H^{(\Lambda)}$ is the underlying quark-gluon subprocess scattering amplitude in which each incident and final hadron is replaced by valence quarks with collinear momenta $k_i^+ = x_i p_H^+$, $\vec{k}_{\perp i} = x_i \vec{p}_{\perp H}$. The invariant mass of all intermediate states in T_H is evaluated above the separation scale $\mathcal{M}_n^2 > \Lambda^2$. The essential part of the hadronic wavefunction is the distribution amplitude,[35] defined as the integral over transverse momenta of the valence (lowest

particle number) Fock wavefunction.

The leading power fall-off of the hard scattering amplitude as given by dimensional counting rules follows from the nominal scaling of the hard-scattering amplitude: $T_H \sim 1/Q^{n-4}$, where n is the total number of fields (quarks, leptons, or gauge fields) participating in the hard scattering.[36),37)] Thus the reaction is dominated by subprocesses and Fock states involving the minimum number of interacting fields. In the case of $2 \to 2$ scattering processes, this implies $d\sigma/dt(AB \to CD) = F_{AB\to CD}(t/s)/s^{n-2}$, where $n = N_A + N_B + N_C + N_D$ and n_H is the minimum number of constituents of H. The near-constancy of the effective QCD coupling at small scales helps explain the empirical success of dimensional counting rules for the near-conformal power law fall-off of form factors and fixed angle scaling.[38)] For example, one sees the onset of perturbative QCD scaling behavior even for exclusive nuclear amplitudes such as deuteron photodisintegration (Here $n = 1+6+3+3 = 13$.) $s^{11}d\sigma/dt(\gamma d \to pn) \sim$ constant at fixed CM angle. The measured deuteron form factor and the deuteron photodisintegration cross section also appear to follow the leading-twist QCD predictions at large momentum transfers in the few GeV region.[41)–43)]

§5. The Conformal Approximation to QCD

As 't Hooft has emphasized at this meeting, it is important to find an analytic and tractable first approximation to QCD. In this talk I will show how conformal symmetry can provide convenient and systematic approximations to QCD in both its perturbative and nonperturbative domains.

5.1. *The Conformal Template*

In the case of perturbation theory, one can use conformal symmetry as a template, systematically correcting for the nonzero QCD β function[21),44),45)] order-by-order in perturbation theory using the Banks-Zaks procedure.[46)] The contributions from the nonzero β function automatically fix the renormalization scale of the running QCD coupling consistent with the renormalization group and the $N_C \to 0$ Abelian limit. After scale setting, the perturbative series has the same form as the conformal series and thus no $n!$ renormalon divergence. The resulting predictions for physical observables are independent of the choice of renormalization scheme.

The near-conformal behavior of QCD is the basis for commensurate scale relations[19)] which relate observables to each other without renormalization scale or scheme ambiguities.[21),44)] One can derive the commensurate scale relation between the effective charges of any two observables by first computing their relation in conformal gauge theory; the effects of the nonzero QCD $\beta-$ function are then taken into account using the BLM method[22)] to set the scales of the respective couplings. An important example is the generalized Crewther relation:[20)] $[1 + \alpha_R(s^*)/\pi]\left[1 - \alpha_{g_1}(Q^2)/\pi\right] = 1$ where the underlying form at zero β function is dictated by conformal symmetry.[47)] Here $\alpha_R(s)/\pi$ and $-\alpha_{g_1}(Q^2)/\pi$ represent the entire radiative corrections to $R_{e^+e^-}(s)$ and the Bjorken sum rule for the $g_1(x, Q^2)$ structure function measured in spin-dependent deep inelastic scattering, respectively.

The relation between s^* and Q^2 can be computed order by order in perturbation theory using the BLM method.[22] The ratio of physical scales guarantees that the effect of new quark thresholds is commensurate. Commensurate scale relations are renormalization-scheme independent and satisfy the group properties of the renormalization group. Each observable can be computed in any convenient renormalization scheme such as dimensional regularization. The $\overline{MS}$ coupling can then be eliminated; it becomes only an intermediary.[19]

5.2. *Scale-Setting for the Three-Gluon Coupling*

Recently Michael Binger and I [48] have analyzed the behavior of the 13 nonzero form factors contributing to the gauge-invariant three-gluon vertex at one-loop, an analysis which is important for heavy quark production and other PQCD processes. Supersymmetric relations between scalar, quark, and gluon loops contributions leads to a simple presentation of the results for a general non-Abelian gauge theories. Only the gluon contribution to the form factors is needed since the massless quark and scalar contributions are inferred from the homogeneous relation $F_G + 4F_Q + (10 - d)F_S = 0$ and the sums $\Sigma_{QG}(F) \equiv (d-2)/2F_Q + F_G$ which are given for each form factor F. The extension to the case of internal masses leads to the modified sum rule $F_{MG} + 4F_{MQ} + (9-d)F_{MS} = 0$. The phenomenology of the three-gluon vertex is largely determined by the form factor multiplying the tree-level tensor. One can define a three-scale effective scale $Q^2_{eff}(p_a^2, p_b^2, p_c^2)$ as a function of the three external virtualities which provides a natural extension of BLM scale setting[22] to the three-gluon vertex. Physical momentum scales thus set the scale of the coupling. The dependence of Q^2_{eff} on the physical scales has a number of surprising features. A complicated threshold and pseudo-threshold behavior is also observed.

In a physical renormalization scheme,[49] gauge couplings are defined directly in terms of physical observables. Such effective charges are analytic functions of the physical scales and their mass thresholds have the correct threshold dependence[50),51] consistent with unitarity. As in QED, heavy particles contribute to physical predictions even at energies below their threshold. This is in contrast to renormalization schemes such as $\overline{MS}$ where mass thresholds are treated as step functions. In the case of supersymmetric grand unification, one finds a number of qualitative differences and improvements in precision over conventional approaches.[51] The analytic threshold corrections can be important in making the measured values of the gauge couplings consistent with unification.

5.3. *AdS/QCD as a First Approximant to Nonperturbative QCD*

The vanishing of the β function at small momentum transfer implies that there is regime where QCD resembles a strongly-coupled theory and mathematical techniques based on conformal invariance can be applied. For example, conformal invariance provides the expansion polynomials for distribution amplitudes,[52)–57] the nonperturbative wavefunctions which control exclusive processes at leading twist.[58),59] One can use the AdS/CFT correspondence between Anti-de Sitter space and conformal gauge theories to obtain an approximation to nonperturbative QCD in the regime where the QCD coupling is large and constant; i.e., one can use the mathe-

matical representation of the conformal group $SO(4,2)$ in five- dimensional anti-de Sitter space to construct a holographic representation to the theory. For example, Guy de Teramond and I [16] have shown that the amplitude $\Phi(z)$ describing the hadronic state in the fifth dimension of Anti-de Sitter space AdS_5 can be precisely mapped to the light-front wavefunctions $\psi_{n/h}$ of hadrons in physical space-time, thus providing a description of hadrons in QCD at the amplitude level. The light-front wavefunctions are relativistic and frame-independent generalizations of the familiar Schrödinger wavefunctions of atomic physics, but they are determined at fixed light-cone time $\tau = t + z/c$—the "front form" advocated by Dirac—rather than at fixed ordinary time t. We derived this correspondence by noticing that the mapping of $z \to \zeta$ analytically transforms the expression for the form factors in AdS/CFT to the exact Drell-Yan-West expression in terms of light-front wavefunctions. An outline of the application of AdS/CFT to QCD is shown in Fig. 1.

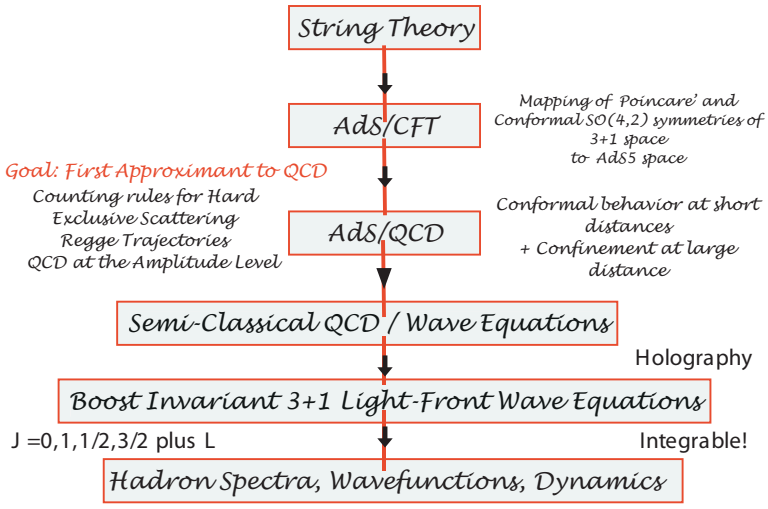

Fig. 1. The AdS/CFT program for QCD.

A key result for mesons is an an effective two-particle light-front radial equation[16),17)]

$$\left[-\frac{d^2}{d\zeta^2} + V(\zeta)\right]\phi(\zeta) = \mathcal{M}^2\phi(\zeta), \tag{5·1}$$

with the effective potential $V(\zeta) \to -(1-4L^2)/4\zeta^2$ the conformal limit. Here $\zeta^2 = x(1-x)\mathbf{b}_\perp^2$ where $x = k^+/P^+$ is the light cone momentum fraction. and $b_\perp$ is the impact separation; i.e. the Fourier conjugate to the relative transverse momentum $k_\perp$. The variable ζ, $0 \le \zeta \le \Lambda_{\rm QCD}^{-1}$, represents the invariant separation between point-like constituents, and it is also the holographic variable z in AdS; *i.e.*, we can identify $\zeta = z$. The solution to (5·1) is $\phi(z) = z^{-\frac{3}{2}}\Phi(z) = Cz^{\frac{1}{2}}J_L(z\mathcal{M})$. This equation reproduces the AdS/CFT solutions. The lowest stable state is determined by the Breitenlohner-Freedman bound.[60)] We can model confinement by imposing Dirichlet boundary conditions at $\phi(z = 1/\Lambda_{\rm QCD}) = 0$. The eigenvalues are then given in terms of the roots of the Bessel functions: $\mathcal{M}_{L,k} = \beta_{L,k}\Lambda_{\rm QCD}$. Alternatively, one

can add a confinement potential $-\kappa^2\zeta^2$ to the effective potential $V(\zeta)$.

With the exception of the pion, the eigenvalues of the effective light-front equation provide a good description of the meson and baryon spectra for light quarks,[61] and its eigensolutions provide a remarkably simple but realistic model of their valence wavefunctions. The resulting normalized light-front wavefunctions for the truncated space model are

$$\widetilde{\psi}_{L,k}(x,\zeta) = B_{L,k}\sqrt{x(1-x)}J_L\left(\zeta\beta_{L,k}\Lambda_{\rm QCD}\right)\theta\big(z \leq \Lambda_{\rm QCD}^{-1}\big), \tag{5·2}$$

where $B_{L,k} = \pi^{-\frac{1}{2}}\Lambda_{\rm QCD}\ J_{1+L}(\beta_{L,k})$. The results display confinement at large interquark separation and conformal symmetry at short distances, thus reproducing dimensional counting rules for hard exclusive processes.

Given the light-front wavefunctions $\psi_{n/H}(x_i, \vec{k}_{\perp i}, \lambda_i)$, one can compute a large range of hadron observables. For example, the valence, sea-quark and gluon distributions are defined from the squares of the LFWFS summed over all Fock states n. Form factors, exclusive weak transition amplitudes[62] such as $B \to \ell\nu\pi$, and the generalized parton distributions[63] measured in deeply virtual Compton scattering are (assuming the "handbag" approximation) overlaps of the initial and final LFWFS with $n = n'$ and $n = n' + 2$. The deeply virtual Compton amplitudes can be Fourier transformed to $b_\perp$ and $\sigma = x^- P^+/2$ space providing new insights into QCD distributions.[64)–67] The distributions in the LF direction σ typically display diffraction patterns arising from the interference of the initial and final state LFWFs .[66),68] This can provide a detailed test of the AdS/CFT LFWFs predictions.

The gauge-invariant distribution amplitude $\phi_H(x_i, Q)$ defined from the integral over the transverse momenta $\vec{k}^2_{\perp i} \leq Q^2$ of the valence (smallest n) Fock state provides a fundamental measure of the hadron at the amplitude level;[58),69] they are the nonperturbative input to the factorized form of hard exclusive amplitudes and exclusive heavy hadron decays in perturbative QCD. The resulting distributions obey the DGLAP and ERBL evolution equations as a function of the maximal invariant mass, thus providing a physical factorization scheme.[35] In each case, the derived quantities satisfy the appropriate operator product expansions, sum rules, and evolution equations. It is interesting to note that the distribution amplitude predicted by AdS/CFT at the hadronic scale is $\phi_\pi(x, Q_0) = (4/\sqrt{3}\pi) f_\pi \sqrt{x(1-x)}$ from both the harmonic oscillator and truncated space models is quite different than the asymptotic distribution amplitude predicted from the PQCD evolution[58] of the pion distribution amplitude: $\phi_\pi(x, Q \to \infty) = \sqrt{3} f_\pi x(1-x)$. The broader shape of the AdS/CFT pion distribution increases the magnitude of the leading-twist perturbative QCD prediction for the pion form factor by a factor of 16/9 compared to the prediction based on the asymptotic form, bringing the PQCD prediction close to the empirical pion form factor.[70]

Hadron form factors can be directly predicted from the overlap integrals in AdS space or equivalently by using the Drell-Yan-West formula in physical space-time. The form factor at high Q^2 receives contributions from small ζ, corresponding to small $\vec{b}_\perp = \mathcal{O}(1/Q)$ (high relative $\vec{k}_\perp = \mathcal{O}(Q)$ as well as $x \to 1$. The AdS/CFT dynamics is thus distinct from endpoint models[71] in which the LFWF is evaluated

solely at small transverse momentum or large impact separation.

The $x \to 1$ endpoint domain of structure functions is often referred to as a "soft" Feynman contribution. In fact $x \to 1$ for the struck quark requires that all of the spectators have $x = k^+/P^+ = (k^0 + k^z)/P^+ \to 0$; this in turn requires high longitudinal momenta $k^z \to -\infty$ for all spectators – unless one has both massless spectator quarks $m \equiv 0$ with zero transverse momentum $k_\perp \equiv 0$, which is a regime of measure zero. If one uses a covariant formalism, such as the Bethe-Salpeter theory, then the virtuality of the struck quark becomes infinitely spacelike: $k_F^2 \sim -(k_\perp^2 + m^2)/(1-x)$ in the endpoint domain. Thus, actually, $x \to 1$ corresponds to high relative longitudinal momentum; it is as hard a domain in the hadron wavefunction as high transverse momentum. Note also that at large x where the struck quark is far-off shell, DGLAP evolution is quenched,[72] so that the fall-off of the DIS cross sections in Q^2 satisfies inclusive-exclusive duality at fixed W^2.

§6. Higher Fock States

Since they are complete and orthonormal, the AdS/CFT model wavefunctions can also be used as a basis for the diagonalization of the full light-front QCD Hamiltonian, thus systematically improving the AdS/CFT approximation. In particular this procedure could provide the higher Fock states of the QCD hadronic eigenstates.

The physics of higher Fock states such as the $|uudq\overline{Q}\rangle$ fluctuation of the proton is clearly nontrivial; the phenomenological distributions display asymmetric $\overline{u}(x) \neq \overline{d}(x)$, and $s(x) \neq \overline{s}(x)$ sea quark distributions, and intrinsic heavy quarks $c\overline{c}$ and $b\overline{b}$ which have their support at high momentum[73] . Color adds an extra element of complexity: for example there are five-different color singlet combinations of six 3_C quark representations which appear in the deuteron's valence wavefunction, leading to the hidden-color phenomena.[74]

6.1. *The Strange Quark Asymmetry*

In the simplest treatment of deep inelastic scattering, nonvalence quarks are produced via gluon splitting and DGLAP evolution. However, in the full theory, heavy quarks are multiply connected to the valence quarks.[75] Although the strange and antistrange distributions in the nucleon are identical when they derive from gluon-splitting $g \to s\overline{s}$, this is not the case when the strange quarks are part of the intrinsic structure of the nucleon – the multiple interactions of the sea quarks produce an asymmetry of the strange and anti-strange distributions in the nucleon due to their different interactions with the other quark constituents. A QED analogy is the distribution of τ^+ and τ^- in a higher Fock state of muonium μ^+e^-. The τ^- is attracted to the higher momentum μ^+ thus asymmetrically distorting its momentum distribution. Similar effects will happen in QCD. If we use the diquark model $|\,p\rangle \sim \left|\,u_{3_c}(ud)_{\overline{3}_C}\right\rangle$, then the Q_{3_C} in the $\left|\,u(ud)Q\overline{Q}\right\rangle$ Fock state will be attracted to the heavy diquark and thus have higher rapidity than the $\overline{Q}$. An alternative model is the $|\,K\Lambda\rangle$ fluctuation model for the $|\,uuds\overline{s}\rangle$ Fock state of the proton.[76] The s quark tends to have higher x.

Empirical evidence continues to accumulate that the strange-antistrange quark

distributions are not symmetric in the proton.[76)–78)] The experimentally observed asymmetry appears to be small but positive: $\int dx x[s(x) - \overline{s}(x)] > 0$. The results of a recent CTEQ global data analysis of neutrino-induced dimuon data are given in ref.[79)] . The shape of the strangeness asymmetry is consistent with the ΛK fluctuation model.[76)] Kretzner[77)] has noted that a significant part of the NuTeV anomaly could be due to this asymmetry, The $\overline{s}(x) - s(x)$ asymmetry can be studied in detail in $p\overline{p}$ collisions by searching for antisymmetric forward-backward strange quark distributions in the $\overline{p} - p$ CM frame.

6.2. *Intrinsic Heavy Quarks*

The probability for Fock states of a light hadron such as the proton to have an extra heavy quark pair decreases as $1/m_Q^2$ in non-Abelian gauge theory.[80),81)] The relevant matrix element is the cube of the QCD field strength $G^3_{\mu\nu}$. This is in contrast to abelian gauge theory where the relevant operator is $F^4_{\mu\nu}$ and the probability of intrinsic heavy leptons in QED bound state is suppressed as $1/m_\ell^4$. The intrinsic Fock state probability is maximized at minimal off-shellness. It is useful to define the transverse mass $m_{\perp i} = \sqrt{k_{\perp i}^2 + m_i^2}$. The maximum probability then occurs at $x_i = m^i_\perp / \sum_{j=1}^n m^j_\perp$; *i.e.*, when the constituents have minimal invariant mass and equal rapidity. Thus the heaviest constituents have the highest momentum fractions and the highest x_i. Intrinsic charm thus predicts that the charm structure function has support at large x_{bj} in excess of DGLAP extrapolations;[75)] this is in agreement with the EMC measurements.[82)] Intrinsic charm can also explain the $J/\psi \to \rho\pi$ puzzle.[83)] It also affects the extraction of suppressed CKM matrix elements in B decays.[84)]

The dissociation of the intrinsic charm $|uudc\overline{c}>$ Fock state of the proton on a nucleus can produce a leading heavy quarkonium state at high $x_F = x_c + x_{\overline{c}}$ in $pA \to J/\psi X A'$ since the c and $\overline{c}$ can readily coalesce into the charmonium state. Since the constituents of a given intrinsic heavy-quark Fock state tend to have the same rapidity, coalescence of multiple partons from the projectile Fock state into charmed hadrons and mesons is also favored. For example, one can produce a leading Λ_c at high x_F and low p_T from the coalescence of the udc constituents of the projectile $|uudc\overline{c}>$ Fock state. A similar coalescence mechanism was used in atomic physics to produce relativistic antihydrogen in $\overline{p}A$ collisions.[85)] This phenomena is important not only for understanding heavy-hadron phenomenology, but also for understanding the sources of neutrinos in astrophysics experiments[86)] and the "long-flying" component in cosmic rays.[87)]

In the case of a nuclear target, the charmonium state will be produced at small transverse momentum and high x_F with a characteristic $A^{2/3}$ nuclear dependence since the color-octet color-octet $|(uud)_{8C}(c\overline{c})_{8C}>$ Fock state interacts on the front surface of the nuclear target.[88)] This forward contribution is in addition to the A^1 contribution derived from the usual perturbative QCD fusion contribution at small x_F. Because of these two components, the cross section violates perturbative QCD factorization for hard inclusive reactions.[89)] This is consistent with the observed two-component cross section for charmonium production observed by the NA3 col-

laboration at CERN[90] and more recent experiments.[91] The diffractive dissociation of the intrinsic charm Fock state leads to leading charm hadron production and fast charmonium production in agreement with measurements.[92] Intrinsic charm can also explain the $J/\psi \to \rho\pi$ puzzle,[83] and it affects the extraction of suppressed CKM matrix elements in B decays.[84]

The production cross section for the double-charm Ξ_{cc}^+ baryon[93] and the production of J/ψ pairs appears to be consistent with the diffractive dissociation and coalescence of double IC Fock states.[94] It is unlikely that the appearance of two heavy quarks at high x_F could be explained by the "color drag model" used in PYTHIA simulations[95] in which the heavy quarks are accelerated from low to high x by the fast valence quarks. These observations provide compelling evidence for the diffractive dissociation of complex off-shell Fock states of the projectile and contradict the traditional view that sea quarks and gluons are always produced perturbatively via DGLAP evolution. It is also conceivable that the observations[96] of Λ_b at high x_F at the ISR in high energy pp collisions could be due to the diffractive dissociation and coalescence of the "intrinsic bottom" $|uudb\overline{b}>$ Fock states of the proton.

Intrinsic heavy quarks can also enhance the production probability of Higgs bosons at hadron colliders from processes such as $gc \to Hc$. It is thus critical for new experiments (HERMES, HERA, COMPASS) to definitively establish the phenomenology of the charm structure function at large x_{bj}. Recently Kopeliovich, Schmidt, Soffer, and I [88] have proposed a novel mechanism for exclusive diffractive Higgs production $pp \to pHp$ in which the Higgs boson carries a significant fraction of the projectile proton momentum. The production mechanism is based on the subprocess $(Q\overline{Q})g \to H$ where the $Q\overline{Q}$ in the $|uudQ\overline{Q}>$ intrinsic heavy quark Fock state has up to 80% of the projectile protons momentum. This process will provide a clear experimental signal for Higgs production due to the small background in this kinematic region.

6.3. *Hidden Color*

In traditional nuclear physics, the deuteron is a bound state of a proton and a neutron where the binding force arise from the exchange of a pion and other mesonic states. However, QCD provides a new perspective:[97),98] six quarks in the fundamental 3_C representation of $SU(3)$ color can combine into five different color-singlet combinations, only one of which corresponds to a proton and neutron. In fact, if the deuteron wavefunction is a proton-neutron bound state at large distances, then as their separation becomes smaller, the QCD evolution resulting from colored gluon exchange introduce four other "hidden color" states into the deuteron wavefunction.[74] The normalization of the deuteron form factor observed at large Q^2,[99] as well as the presence of two mass scales in the scaling behavior of the reduced deuteron form factor,[97] thus suggest sizable hidden-color Fock state contributions such as $|\,(uud)_{8_C}(ddu)_{8_C}\rangle$ with probability of order 15% in the deuteron wavefunction.[100]

The hidden color states of the deuteron can be materialized at the hadron level as $\Delta^{++}(uuu)\Delta^{-}(ddd)$ and other novel quantum fluctuations of the deuteron. These dual hadron components become more and more important as one probes the deuteron at short distances, such as in exclusive reactions at large momentum trans-

fer. For example, the ratio $d\sigma/dt(\gamma d \to \Delta^{++}\Delta^{-})/d\sigma/dt(\gamma d \to np)$ should increase dramatically with increasing transverse momentum p_T. Similarly the Coulomb dissociation of the deuteron into various exclusive channels $ed \to e' + pn, pp\pi^-, \Delta\Delta, \cdots$ should have a changing composition as the final-state hadrons are probed at high transverse momentum, reflecting the onset of hidden color degrees of freedom.

§7. Diffractive Deep Inelastic Scattering

A remarkable feature of deep inelastic lepton-proton scattering at HERA is that approximately 10% events are diffractive:[101),102)] the target proton remains intact, and there is a large rapidity gap between the proton and the other hadrons in the final state. These diffractive deep inelastic scattering (DDIS) events can be understood most simply from the perspective of the color-dipole model: the $q\overline{q}$ Fock state of the high-energy virtual photon diffractively dissociates into a diffractive dijet system. The exchange of multiple gluons between the color dipole of the $q\overline{q}$ and the quarks of the target proton neutralizes the color separation and leads to the diffractive final state. The same multiple gluon exchange also controls diffractive vector meson electroproduction at large photon virtuality.[103)] This observation presents a paradox: if one chooses the conventional parton model frame where the photon light-front momentum is negative $q+ = q^0 + q^z < 0$, the virtual photon interacts with a quark constituent with light-cone momentum fraction $x = k^+/p^+ = x_{bj}$. Furthermore, the gauge link associated with the struck quark (the Wilson line) becomes unity in light-cone gauge $A^+ = 0$. Thus the struck "current" quark apparently experiences no final-state interactions. Since the light-front wavefunctions $\psi_n(x_i, k_{\perp i})$ of a stable hadron are real, it appears impossible to generate the required imaginary phase associated with pomeron exchange, let alone large rapidity gaps.

This paradox was resolved by Hoyer, Marchal, Peigne, Sannino and myself.[104)] Consider the case where the virtual photon interacts with a strange quark—the $s\overline{s}$ pair is assumed to be produced in the target by gluon splitting. In the case of Feynman gauge, the struck s quark continues to interact in the final state via gluon exchange as described by the Wilson line. The final-state interactions occur at a light-cone time $\Delta\tau \simeq 1/\nu$ shortly after the virtual photon interacts with the struck quark. When one integrates over the nearly-on-shell intermediate state, the amplitude acquires an imaginary part. Thus the rescattering of the quark produces a separated color-singlet $s\overline{s}$ and an imaginary phase. In the case of the light-cone gauge $A^+ = \eta \cdot A = 0$, one must also consider the final-state interactions of the (unstruck) $\overline{s}$ quark. The gluon propagator in light-cone gauge $d^{\mu\nu}_{LC}(k) = (i/k^2 + i\epsilon)\,[-g^{\mu\nu} + (\eta^\mu k^\nu + k^\mu \eta^\nu/\eta \cdot k)]$ is singular at $k^+ = \eta \cdot k = 0$. The momentum of the exchanged gluon k^+ is of $\mathcal{O}(1/\nu)$; thus rescattering contributes at leading twist even in light-cone gauge. The net result is gauge invariant and is identical to the color dipole model calculation. The calculation of the rescattering effects on DIS in Feynman and light-cone gauge through three loops is given in detail for an Abelian model in the references.[104)] The result shows that the rescattering corrections reduce the magnitude of the DIS cross section in analogy to nuclear shadowing.

A new understanding of the role of final-state interactions in deep inelastic scat-

tering has thus emerged. The multiple scattering of the struck parton via instantaneous interactions in the target generates dominantly imaginary diffractive amplitudes, giving rise to an effective "hard pomeron" exchange. The presence of a rapidity gap between the target and diffractive system requires that the target remnant emerges in a color-singlet state; this is made possible in any gauge by the soft rescattering. The resulting diffractive contributions leave the target intact and do not resolve its quark structure; thus there are contributions to the DIS structure functions which cannot be interpreted as parton probabilities;[104] the leading-twist contribution to DIS from rescattering of a quark in the target is a coherent effect which is not included in the light-front wave functions computed in isolation. One can augment the light-front wave functions with a gauge link corresponding to an external field created by the virtual photon $q\overline{q}$ pair current.[105),106] Such a gauge link is process dependent,[107] so the resulting augmented LFWFs are not universal.[104),105),108] We also note that the shadowing of nuclear structure functions is due to the destructive interference between multi-nucleon amplitudes involving diffractive DIS and on-shell intermediate states with a complex phase. In contrast, the wave function of a stable target is strictly real since it does not have on-energy-shell intermediate state configurations. The physics of rescattering and shadowing is thus not included in the nuclear light-front wave functions, and a probabilistic interpretation of the nuclear DIS cross section is precluded.

Rikard Enberg, Paul Hoyer, Gunnar Ingelman and I[109] have shown that the quark structure function of the effective hard pomeron has the same form as the quark contribution of the gluon structure function. The hard pomeron is not an intrinsic part of the proton; rather it must be considered as a dynamical effect of the lepton-proton interaction. Our QCD-based picture also applies to diffraction in hadron-initiated processes. The rescattering is different in virtual photon- and hadron-induced processes due to the different color environment, which accounts for the observed non-universality of diffractive parton distributions. This framework also provides a theoretical basis for the phenomenologically successful Soft Color Interaction (SCI) model[110] which includes rescattering effects and thus generates a variety of final states with rapidity gaps.

§8. Single-Spin Asymmetries from Final-State Interactions

Among the most interesting polarization effects are single-spin azimuthal asymmetries in semi-inclusive deep inelastic scattering, representing the correlation of the spin of the proton target and the virtual photon to hadron production plane: $\vec{S}_p \cdot \vec{q} \times \vec{p}_H$. Such asymmetries are time-reversal odd, but they can arise in QCD through phase differences in different spin amplitudes. In fact, final-state interactions from gluon exchange between the outgoing quarks and the target spectator system lead to single-spin asymmetries in semi-inclusive deep inelastic lepton-proton scattering which are not power-law suppressed at large photon virtuality Q^2 at fixed x_{bj}.[111] In contrast to the SSAs arising from transversity and the Collins fragmentation function, the fragmentation of the quark into hadrons is not necessary; one predicts a correlation with the production plane of the quark jet itself. Physically, the

final-state interaction phase arises as the infrared-finite difference of QCD Coulomb phases for hadron wave functions with differing orbital angular momentum. The same proton matrix element which determines the spin-orbit correlation $\vec{S} \cdot \vec{L}$ also produces the anomalous magnetic moment of the proton, the Pauli form factor, and the generalized parton distribution E which is measured in deeply virtual Compton scattering. Thus the contribution of each quark current to the SSA is proportional to the contribution $\kappa_{q/p}$ of that quark to the proton target's anomalous magnetic moment $\kappa_p = \sum_q e_q \kappa_{q/p}$.[111),112)] The HERMES collaboration has recently measured the SSA in pion electroproduction using transverse target polarization.[113)] The Sivers and Collins effects can be separated using planar correlations; both contributions are observed to contribute, with values not in disagreement with theory expectations.[113),114)] A related analysis also predicts that the initial-state interactions from gluon exchange between the incoming quark and the target spectator system lead to leading-twist single-spin asymmetries in the Drell-Yan process $H_1 H_2^{\uparrow} \to \ell^+ \ell^- X$.[107),115)] The SSA in the Drell-Yan process is the same as that obtained in SIDIS, with the appropriate identification of variables, but with the opposite sign. There is no Sivers effect in charged-current reactions since the W only couples to left-handed quarks.[116)]

If both the quark and antiquark in the initial state of the Drell-Yan subprocess $q\overline{q}\mu^+\mu^-$ interact with the spectators of the other incident hadron, one finds a breakdown of the Lam-Tung relation, which was formerly believed to be a general prediction of leading-twist QCD. These double initial-state interactions also lead to a $\cos 2\phi$ planar correlation in unpolarized Drell-Yan reactions.[117)] More generally one must consider subprocesses involving initial-state gluons such as $ngq\overline{q} \to \ell\overline{\ell}$ in addition to subprocesses with extra final-state gluons.

The final-state interaction mechanism provides an appealing physical explanation within QCD of single-spin asymmetries. Remarkably, the same matrix element which determines the spin-orbit correlation $\vec{S} \cdot \vec{L}$ also produces the anomalous magnetic moment of the proton, the Pauli form factor, and the generalized parton distribution E which is measured in deeply virtual Compton scattering. Physically, the final-state interaction phase arises as the infrared-finite difference of QCD Coulomb phases for hadron wave functions with differing orbital angular momentum. An elegant discussion of the Sivers effect including its sign has been given by Burkardt.[112)] As shown recently by Gardner and myself,[118)] one can also use the Sivers effect to study the orbital angular momentum of gluons by tagging a gluon jet in semi-inclusive DIS. In this case, the final-state interactions are enhanced by the large color charge of the gluons.

The final-state interaction effects can also be identified with the gauge link which is present in the gauge-invariant definition of parton distributions.[106)] Even when the light-cone gauge is chosen, a transverse gauge link is required. Thus in any gauge the parton amplitudes need to be augmented by an additional eikonal factor incorporating the final-state interaction and its phase.[105),119)] The net effect is that it is possible to define transverse momentum dependent parton distribution functions which contain the effect of the QCD final-state interactions.

§9. Diffraction Dissociation as a Tool to Resolve Hadron Substructure and Test Color Transparency

Diffractive multi-jet production in heavy nuclei provides a novel way to resolve the shape of light-front Fock state wave functions and test color transparency.[120] For example, consider the reaction[121),122)] $\pi A \to \mathrm{Jet}_1 + \mathrm{Jet}_2 + A'$ at high energy where the nucleus A' is left intact in its ground state. The transverse momenta of the jets balance so that $\vec{k}_{\perp i} + \vec{k}_{\perp 2} = \vec{q}_\perp < {R^{-1}}_A$. Because of color transparency, the valence wave function of the pion with small impact separation will penetrate the nucleus with minimal interactions, diffracting into jet pairs.[121)] The $x_1 = x$, $x_2 = 1 - x$ dependence of the dijet distributions will thus reflect the shape of the pion valence light-cone wave function in x; similarly, the $\vec{k}_{\perp 1} - \vec{k}_{\perp 2}$ relative transverse momenta of the jets gives key information on the second transverse momentum derivative of the underlying shape of the valence pion wavefunction.[122),123)] The diffractive nuclear amplitude extrapolated to $t = 0$ should be linear in nuclear number A if color transparency is correct. The integrated diffractive rate will then scale as $A^2/R_A^2 \sim A^{4/3}$. This is in fact what has been observed by the E791 collaboration at FermiLab for 500 GeV incident pions on nuclear targets.[124)] The measured momentum fraction distribution of the jets with high transverse momentum is found to be approximately consistent with the shape of the pion asymptotic distribution amplitude, $\phi_\pi^{\mathrm{asympt}}(x) = \sqrt{3} f_\pi x(1-x)$;[125)] however, there is an indication from the data that the distribution is broader at lower transverse momentum, consistent with the AdS/CFT prediction.

Color transparency, as evidenced by the Fermilab measurements of diffractive dijet production, implies that a pion can interact coherently throughout a nucleus with minimal absorption, in dramatic contrast to traditional Glauber theory based on a fixed $\sigma_{\pi n}$ cross section. Color transparency gives direct validation of the gauge interactions of QCD. Color transparency has also been observed in diffractive electroproduction of ρ mesons[126)] and in quasi-elastic $pA \to pp(A-1)$ scattering[127)] where only the small size fluctuations of the hadron wavefunction enters the hard exclusive scattering amplitude. In the latter case an anomaly occurs at $\sqrt{s} \simeq 5$ GeV, most likely signaling a resonance effect at the charm threshold.[128)]

§10. Shadowing and Antishadowing of Nuclear Structure Functions

One of the novel features of QCD involving nuclei is the *antishadowing* of the nuclear structure functions which is observed in deep inelastic lepton scattering and other hard processes. Empirically, one finds $R_A(x,Q^2) \equiv \big(F_{2A}(x,Q^2)/(A/2)F_d(x,Q^2)\big) > 1$ in the domain $0.1 < x < 0.2$; *i.e.*, the measured nuclear structure function (referenced to the deuteron) is larger than than the scattering on a set of A independent nucleons.

The shadowing of the nuclear structure functions: $R_A(x,Q^2) < 1$ at small $x < 0.1$ can be readily understood in terms of the Gribov-Glauber theory. Consider a two-step process in the nuclear target rest frame. The incoming $q\overline{q}$ dipole first interacts diffractively $\gamma^* N_1 \to (q\overline{q})N_1$ on nucleon N_1 leaving it intact. This is the

leading-twist diffractive deep inelastic scattering (DDIS) process which has been measured at HERA to constitute approximately 10% of the DIS cross section at high energies. The $q\overline{q}$ state then interacts inelastically on a downstream nucleon N_2 : $(q\overline{q})N_2 \to X$. The phase of the pomeron-dominated DDIS amplitude is close to imaginary, and the Glauber cut provides another phase i, so that the two-step process has opposite phase and destructively interferes with the one-step DIS process $\gamma * N_2 \to X$ where N_1 acts as an unscattered spectator. The one-step and-two step amplitudes can coherently interfere as long as the momentum transfer to the nucleon N_1 is sufficiently small that it remains in the nuclear target; *i.e.*, the Ioffe length[129] $L_I = 2M\nu/Q^2$ is large compared to the inter-nucleon separation. In effect, the flux reaching the interior nucleons is diminished, thus reducing the number of effective nucleons and $R_A(x, Q^2) < 1$.

There are also leading-twist diffractive contributions $\gamma^* N_1 \to (q\overline{q})N_1$ arising from Reggeon exchanges in the t-channel.[130] For example, isospin–non-singlet $C = +$ Reggeons contribute to the difference of proton and neutron structure functions, giving the characteristic Kuti-Weisskopf $F_{2p} - F_{2n} \sim x^{1-\alpha_R(0)} \sim x^{0.5}$ behavior at small x. The x dependence of the structure functions reflects the Regge behavior $\nu^{\alpha_R(0)}$ of the virtual Compton amplitude at fixed Q^2 and $t = 0$. The phase of the diffractive amplitude is determined by analyticity and crossing to be proportional to $-1 + i$ for $\alpha_R = 0.5$, which together with the phase from the Glauber cut, leads to *constructive* interference of the diffractive and nondiffractive multi-step nuclear amplitudes. Furthermore, because of its x dependence, the nuclear structure function is enhanced precisely in the domain $0.1 < x < 0.2$ where antishadowing is empirically observed. The strength of the Reggeon amplitudes is fixed by the fits to the nucleon structure functions, so there is little model dependence.

As noted above, the Bjorken-scaling diffractive contribution to DIS arises from the rescattering of the struck quark after it is struck (in the parton model frame $q^+ \leq 0$), an effect induced by the Wilson line connecting the currents. Thus one cannot attribute DDIS to the physics of the target nucleon computed in isolation.[104] Similarly, since shadowing and antishadowing arise from the physics of diffraction, we cannot attribute these phenomena to the structure of the nucleus itself: shadowing and antishadowing arise because of the $\gamma^* A$ collision and the history of the $q\overline{q}$ dipole as it propagates through the nucleus.

Ivan Schmidt, Jian-Jun Yang, and I[131] have extended the Glauber analysis to the shadowing and antishadowing of all of the electroweak structure functions. Quarks of different flavors will couple to different Reggeons; this leads to the remarkable prediction that nuclear antishadowing is not universal; it depends on the quantum numbers of the struck quark. This picture leads to substantially different antishadowing for charged and neutral current reactions, thus affecting the extraction of the weak-mixing angle θ_W. We find that part of the anomalous NuTeV result[132] for θ_W could be due to the non-universality of nuclear antishadowing for charged and neutral currents. Detailed measurements of the nuclear dependence of individual quark structure functions are thus needed to establish the distinctive phenomenology of shadowing and antishadowing and to make the NuTeV results definitive. Schmidt, Yang, and I have also identified contributions to the nuclear

multi-step reactions which arise from odderon exchange and hidden color degrees of freedom in the nuclear wavefunction. There are other ways in which this new view of antishadowing can be tested; antishadowing can also depend on the target and beam polarization.

§11. Higher Twist Effects

Although the contributions of higher twist processes are suppressed at high transverse momentum, there are some areas of phenomenology where they can play a dominant role. For example, hadrons can interact directly within a hard subprocess, leading to higher twist contributions which can actually dominate over leading twist processes.[133),134)] A classic example is the reaction $\pi q \to \ell^+\ell^- q'$ which dominates Drell-Yan reactions $\pi N \to \ell^+\ell^- X$ at high x_F and produces longitudinally polarized lepton pairs.

Higher-twist reactions[135)] such as $uu \to p\overline{d}$ and $(uud)u \to pu$ can dominate single inclusive hadron reactions at high transverse momentum such as $pp \to pX$ at high $x_T = 2p_T/\sqrt{s}$. Such "direct" reactions can explain the fast-falling power-law falloffs observed at fixed x_T and fixed θ_{cm} observed at the ISR, FermiLab and RHIC. A review of the fixed x_T scaling data is given in ref.[135)]

Acknowledgments

I thank the organizers of the Sakata Jubilee for their invitation to speak at this meeting. I also thank my collaborators for many helpful discussions. This work was supported in part by the Department of Energy, contract No. DE-AC02-76SF00515.

References

1) S. Sakata, Prog. Theor. Phys. **16**, 686 (1956).
2) M. Breidenbach *et al.*, Phys. Rev. Lett. **23**, 935 (1969).
3) J. D. Bjorken, Phys. Rev. **179**, 1547 (1969).
4) M. Gell-Mann, Phys. Rev. **125**, 1067 (1962).
5) Y. Ne'eman, Nucl. Phys. **26**, 222 (1961).
6) G. Zweig, CERN-8419-TH-412 (1964); Reprinted in Development in the Quark Theory of Hadrons, A Reprint Collection V.1: 1964-1978, ed. D. B. Lichtenberg and S. P. Rosen, Hadronic Press, Inc., Monamtum, Mass. (1980) 22.
7) J. D. Bjorken and E. A. Paschos, Phys. Rev. **185**, 1975 (1969).
8) S. D. Drell, D. J. Levy and T. M. Yan, Phys. Rev. Lett. **22**, 744 (1969).
9) O. W. Greenberg, Phys. Rev. Lett. **13**, 598 (1964).
10) H. Fritzsch, M. Gell-Mann and H. Leutwyler, Phys. Lett. B **47**, 365 (1973).
11) C. N. Yang and R. L. Mills, Phys. Rev. **96**, 191 (1954).
12) M. Y. Han and Y. Nambu, Phys. Rev. **139**, B1006 (1965).
13) J. H. Field, LPNHE-84-04 (1984).
14) J. W. Harris, Czech. J. Phys. **55**, B297 (2005).
15) J. M. Maldacena, Adv. Theor. Math. Phys. **2**, 231 (1998) [Int. J. Theor. Phys. **38**, 1113 (1999)] [arXiv:hep-th/9711200].
16) S. J. Brodsky, arXiv:hep-ph/0610115.
17) S. J. Brodsky and G. F. de Teramond, SLAC-PUB-12361 (2007).
18) S. J. Brodsky and J. Rathsman, arXiv:hep-ph/9906339.
19) S. J. Brodsky and H. J. Lu, Phys. Rev. D **51**, 3652 (1995) [arXiv:hep-ph/9405218].
20) S. J. Brodsky, G. T. Gabadadze, A. L. Kataev and H. J. Lu, Phys. Lett. B **372**, 133 (1996)

[arXiv:hep-ph/9512367].
21) S. J. Brodsky, E. Gardi, G. Grunberg and J. Rathsman, Phys. Rev. D **63**, 094017 (2001) [arXiv:hep-ph/0002065].
22) S. J. Brodsky, G. P. Lepage and P. B. Mackenzie, Phys. Rev. D **28**, 228 (1983).
23) S. J. Brodsky and H. J. Lu, arXiv:hep-ph/9211308.
24) E. C. G. Stueckelberg and A. Petermann, Helv. Phys. Acta **26**, 499 (1953).
25) S. J. Brodsky and P. Huet, Phys. Lett. B **417**, 145 (1998) [arXiv:hep-ph/9707543].
26) L. von Smekal, R. Alkofer and A. Hauck, Phys. Rev. Lett. **79**, 3591 (1997) [arXiv:hep-ph/9705242].
27) D. Zwanziger, Phys. Rev. D **69**, 016002 (2004) [arXiv:hep-ph/0303028].
28) A. C. Mattingly and P. M. Stevenson, Phys. Rev. D **49**, 437 (1994) [arXiv:hep-ph/9307266].
29) S. J. Brodsky, S. Menke, C. Merino and J. Rathsman, Phys. Rev. D **67**, 055008 (2003) [arXiv:hep-ph/0212078].
30) M. Baldicchi and G. M. Prosperi, Phys. Rev. D **66**, 074008 (2002) [arXiv:hep-ph/0202172].
31) S. J. Brodsky, J. R. Pelaez and N. Toumbas, Phys. Rev. D **60**, 037501 (1999) [arXiv:hep-ph/9810424].
32) S. Furui and H. Nakajima, Few Body Syst. **40**, 101 (2006) [arXiv:hep-lat/0612009].
33) D. Antonov and H. J. Pirner, arXiv:hep-ph/0702227.
34) G. Parisi, Phys. Lett. B **39**, 643 (1972).
35) G. P. Lepage and S. J. Brodsky, Phys. Rev. D **22**, 2157 (1980).
36) S. J. Brodsky and G. R. Farrar, Phys. Rev. D **11**, 1309 (1975).
37) V. A. Matveev, R. M. Muradian and A. N. Tavkhelidze, Lett. Nuovo Cim. **7**, 719 (1973).
38) S. J. Brodsky and G. P. Lepage, Adv. Ser. Direct. High Energy Phys. **5**, 93 (1989).
39) S. J. Brodsky, C. R. Ji, A. Pang and D. G. Robertson, Phys. Rev. D **57**, 245 (1998) [arXiv:hep-ph/9705221].
40) B. Melic, B. Nizic and K. Passek, Phys. Rev. D **65**, 053020 (2002) [arXiv:hep-ph/0107295].
41) R. J. Holt, Phys. Rev. C **41**, 2400 (1990).
42) C. Bochna *et al.* [E89-012 Collaboration], Phys. Rev. Lett. **81**, 4576 (1998) [arXiv:nucl-ex/9808001].
43) P. Rossi *et al.* [CLAS Collaboration], arXiv:hep-ph/0405207.
44) J. Rathsman, in *Proc. of the 5th International Symposium on Radiative Corrections (RADCOR 2000)* ed. Howard E. Haber, arXiv:hep-ph/0101248.
45) G. Grunberg, JHEP **0108**, 019 (2001) [arXiv:hep-ph/0104098].
46) T. Banks and A. Zaks, Nucl. Phys. B **196**, 189 (1982).
47) R. J. Crewther, Phys. Rev. Lett. **28**, 1421 (1972).
48) M. Binger and S. J. Brodsky, Phys. Rev. D **74**, 054016 (2006) [arXiv:hep-ph/0602199].
49) G. Grunberg, Phys. Rev. D **29**, 2315 (1984).
50) S. J. Brodsky, M. S. Gill, M. Melles and J. Rathsman, Phys. Rev. D **58**, 116006 (1998) [arXiv:hep-ph/9801330].
51) M. Binger and S. J. Brodsky, Phys. Rev. D **69**, 095007 (2004) [arXiv:hep-ph/0310322].
52) S. J. Brodsky, Y. Frishman, G. P. Lepage and C. T. Sachrajda, Phys. Lett. B **91**, 239 (1980).
53) S. J. Brodsky, P. Damgaard, Y. Frishman and G. P. Lepage, Phys. Rev. D **33**, 1881 (1986).
54) S. J. Brodsky, Y. Frishman and G. P. Lepage, Phys. Lett. B **167**, 347 (1986).
55) V. M. Braun, G. P. Korchemsky and D. Mueller, Prog. Part. Nucl. Phys. **51**, 311 (2003) [arXiv:hep-ph/0306057].
56) S. J. Brodsky, arXiv:hep-ph/0408069.
57) S. J. Brodsky, SLAC-PUB-10206 (2003).
58) G. P. Lepage and S. J. Brodsky, Phys. Lett. B **87**, 359 (1979).
59) S. J. Brodsky, SLAC-PUB-8649 (2000).
60) P. Breitenlohner and D. Z. Freedman, Annals Phys. **144**, 249 (1982).
61) S. J. Brodsky and G. F. de Teramond, AIP Conf. Proc. **814**, 108 (2006) [arXiv:hep-ph/0510240].
62) S. J. Brodsky and D. S. Hwang, Nucl. Phys. B **543**, 239 (1999) [arXiv:hep-ph/9806358].
63) S. J. Brodsky, M. Diehl and D. S. Hwang, Nucl. Phys. B **596**, 99 (2001) [arXiv:hep-ph/0009254].
64) M. Burkardt, Int. J. Mod. Phys. A **21**, 926 (2006) [arXiv:hep-ph/0509316].
65) X. d. Ji, Phys. Rev. Lett. **91**, 062001 (2003) [arXiv:hep-ph/0304037].

66) S. J. Brodsky, D. Chakrabarti, A. Harindranath, A. Mukherjee and J. P. Vary, Phys. Lett. B **641**, 440 (2006) [arXiv:hep-ph/0604262].
67) P. Hoyer, arXiv:hep-ph/0608295.
68) S. J. Brodsky, D. Chakrabarti, A. Harindranath, A. Mukherjee and J. P. Vary, Phys. Rev. D **75**, 014003 (2007) [arXiv:hep-ph/0611159].
69) A. V. Efremov and A. V. Radyushkin, Phys. Lett. B **94**, 245 (1980).
70) H. M. Choi and C. R. Ji, Phys. Rev. D **74**, 093010 (2006) [arXiv:hep-ph/0608148].
71) A. V. Radyushkin, Phys. Lett. B **642**, 459 (2006) [arXiv:hep-ph/0605116].
72) S. J. Brodsky and G. P. Lepage, C79/02/13-1 (1979).
73) S. J. Brodsky, arXiv:hep-ph/0004211.
74) S. J. Brodsky, C. R. Ji and G. P. Lepage, Phys. Rev. Lett. **51**, 83 (1983).
75) S. J. Brodsky, P. Hoyer, C. Peterson and N. Sakai, Phys. Lett. B **93**, 451 (1980).
76) S. J. Brodsky and B. Q. Ma, Phys. Lett. B **381**, 317 (1996) [arXiv:hep-ph/9604393].
77) S. Kretzer, arXiv:hep-ph/0408287.
78) B. Portheault, arXiv:hep-ph/0406226.
79) F. Olness *et al.*, Eur. Phys. J. C **40**, 145 (2005) [arXiv:hep-ph/0312323].
80) M. Franz, M. V. Polyakov and K. Goeke, Phys. Rev. D **62**, 074024 (2000) [arXiv:hep-ph/0002240].
81) S. J. Brodsky, J. C. Collins, S. D. Ellis, J. F. Gunion and A. H. Mueller, C84/06/23 (1984).
82) B. W. Harris, J. Smith and R. Vogt, Nucl. Phys. B **461**, 181 (1996) [arXiv:hep-ph/9508403].
83) S. J. Brodsky and M. Karliner, Phys. Rev. Lett. **78**, 4682 (1997) [arXiv:hep-ph/9704379].
84) S. J. Brodsky and S. Gardner, Phys. Rev. D **65**, 054016 (2002) [arXiv:hep-ph/0108121].
85) C. T. Munger, S. J. Brodsky and I. Schmidt, Phys. Rev. D **49**, 3228 (1994).
86) F. Halzen, Nucl. Phys. Proc. Suppl. **136**, 93 (2004) [Acta Phys. Polon. B **36**, 481 (2005 APCPC,745,3-13.2005 NUPHA,A752,3-13.2005)] [arXiv:astro-ph/0402083].
87) I. M. Dremin and V. I. Yakovlev, Astropart. Phys. **26**, 1 (2006) [arXiv:hep-ph/0510377].
88) S. J. Brodsky, B. Kopeliovich, I. Schmidt and J. Soffer, Phys. Rev. D **73**, 113005 (2006) [arXiv:hep-ph/0603238].
89) P. Hoyer, M. Vanttinen and U. Sukhatme, Phys. Lett. B **246**, 217 (1990).
90) J. Badier *et al.* [NA3 Collaboration], Phys. Lett. B **104**, 335 (1981).
91) M. J. Leitch *et al.* [FNAL E866/NuSea collaboration], Phys. Rev. Lett. **84**, 3256 (2000) [arXiv:nucl-ex/9909007].
92) J. C. Anjos, J. Magnin and G. Herrera, Phys. Lett. B **523**, 29 (2001) [arXiv:hep-ph/0109185].
93) A. Ocherashvili *et al.* [SELEX Collaboration], Phys. Lett. B **628**, 18 (2005) [arXiv:hep-ex/0406033].
94) R. Vogt and S. J. Brodsky, Phys. Lett. B **349**, 569 (1995) [arXiv:hep-ph/9503206].
95) B. Andersson, G. Gustafson, G. Ingelman and T. Sjostrand, Phys. Rept. **97**, 31 (1983).
96) G. Bari *et al.*, Nuovo Cim. A **104**, 1787 (1991).
97) S. J. Brodsky and B. T. Chertok, Phys. Rev. D **14**, 3003 (1976).
98) V. A. Matveev and P. Sorba, Lett. Nuovo Cim. **20**, 435 (1977).
99) R. G. Arnold *et al.*, Phys. Rev. Lett. **35**, 776 (1975).
100) G. R. Farrar, K. Huleihel and H. y. Zhang, Phys. Rev. Lett. **74**, 650 (1995).
101) C. Adloff *et al.* [H1 Collaboration], Z. Phys. C **76**, 613 (1997) [arXiv:hep-ex/9708016].
102) J. Breitweg *et al.* [ZEUS Collaboration], Eur. Phys. J. C **6**, 43 (1999) [arXiv:hep-ex/9807010].
103) S. J. Brodsky, L. Frankfurt, J. F. Gunion, A. H. Mueller and M. Strikman, Phys. Rev. D **50**, 3134 (1994) [arXiv:hep-ph/9402283].
104) S. J. Brodsky, P. Hoyer, N. Marchal, S. Peigne and F. Sannino, Phys. Rev. D **65**, 114025 (2002) [arXiv:hep-ph/0104291].
105) A. V. Belitsky, X. Ji and F. Yuan, Nucl. Phys. B **656**, 165 (2003) [arXiv:hep-ph/0208038].
106) J. C. Collins and A. Metz, Phys. Rev. Lett. **93**, 252001 (2004) [arXiv:hep-ph/0408249].
107) J. C. Collins, Phys. Lett. B **536**, 43 (2002) [arXiv:hep-ph/0204004].
108) J. C. Collins, Acta Phys. Polon. B **34**, 3103 (2003) [arXiv:hep-ph/0304122].
109) S. J. Brodsky, R. Enberg, P. Hoyer and G. Ingelman, Phys. Rev. D **71**, 074020 (2005) [arXiv:hep-ph/0409119].
110) A. Edin, G. Ingelman and J. Rathsman, Phys. Lett. B **366**, 371 (1996) [arXiv:hep-ph/9508386].

111) S. J. Brodsky, D. S. Hwang and I. Schmidt, Phys. Lett. B **530**, 99 (2002) [arXiv:hep-ph/0201296].
112) M. Burkardt, Nucl. Phys. Proc. Suppl. **141**, 86 (2005) [arXiv:hep-ph/0408009].
113) A. Airapetian *et al.* [HERMES Collaboration], Phys. Rev. Lett. **94**, 012002 (2005) [arXiv:hep-ex/0408013].
114) H. Avakian and L. Elouadrhiri [CLAS Collaboration], AIP Conf. Proc. **698**, 612 (2004).
115) S. J. Brodsky, D. S. Hwang and I. Schmidt, Nucl. Phys. B **642**, 344 (2002) [arXiv:hep-ph/0206259].
116) S. J. Brodsky, D. S. Hwang and I. Schmidt, Phys. Lett. B **553**, 223 (2003) [arXiv:hep-ph/0211212].
117) D. Boer, S. J. Brodsky and D. S. Hwang, Phys. Rev. D **67**, 054003 (2003) [arXiv:hep-ph/0211110].
118) S. J. Brodsky and S. Gardner, Phys. Lett. B **643**, 22 (2006) [arXiv:hep-ph/0608219].
119) X. D. Ji and F. Yuan, Phys. Lett. B **543**, 66 (2002) [arXiv:hep-ph/0206057].
120) S. J. Brodsky and A. H. Mueller, Phys. Lett. B **206**, 685 (1988).
121) G. Bertsch, S. J. Brodsky, A. S. Goldhaber and J. F. Gunion, Phys. Rev. Lett. **47**, 297 (1981).
122) L. Frankfurt, G. A. Miller and M. Strikman, Found. Phys. **30**, 533 (2000) [arXiv:hep-ph/9907214].
123) N. N. Nikolaev, W. Schafer and G. Schwiete, Phys. Rev. D **63**, 014020 (2001) [arXiv:hep-ph/0009038].
124) E. M. Aitala *et al.* [E791 Collaboration], Phys. Rev. Lett. **86**, 4773 (2001) [arXiv:hep-ex/0010044].
125) E. M. Aitala *et al.* [E791 Collaboration], Phys. Rev. Lett. **86**, 4768 (2001) [arXiv:hep-ex/0010043].
126) A. B. Borisov [HERMES Collaboration], Nucl. Phys. A **711**, 269 (2002).
127) J. L. S. Aclander *et al.*, Phys. Rev. C **70**, 015208 (2004) [arXiv:nucl-ex/0405025].
128) S. J. Brodsky and G. F. de Teramond, Phys. Rev. Lett. **60**, 1924 (1988).
129) B. L. Ioffe, Phys. Lett. B **30**, 123 (1969).
130) S. J. Brodsky and H. J. Lu, Phys. Rev. Lett. **64**, 1342 (1990).
131) S. J. Brodsky, I. Schmidt and J. J. Yang, Phys. Rev. D **70**, 116003 (2004) [arXiv:hep-ph/0409279].
132) G. P. Zeller *et al.* [NuTeV Collaboration], Phys. Rev. Lett. **88**, 091802 (2002) [Erratum-ibid. **90**, 239902 (2003)] [arXiv:hep-ex/0110059].
133) E. L. Berger and S. J. Brodsky, Phys. Rev. Lett. **42**, 940 (1979).
134) E. L. Berger and S. J. Brodsky, Phys. Rev. D **24**, 2428 (1981).
135) S. J. Brodsky, H. J. Pirner and J. Raufeisen, Phys. Lett. B **637**, 58 (2006) [arXiv:hep-ph/0510315].